Materials and Design 121 (2017) 24–35

Contents lists available at ScienceDirect

Materials and Design

journal homepage: www.elsevier.com/locate/matdes

Correlation between alpha phase morphology and tensile properties of a new beta titanium alloy

S. Sadeghpour [a,b,*], S.M. Abbasi [a], M. Morakabati [a], S. Bruschi [b]

[a] Metallic Materials Research Center, Malek Ashtar University of Technology, Tehran, Iran
[b] University of Padua, Industrial Engineering Department, Via Venezia, 1, Padova 35131, Italy

HIGHLIGHTS

- A novel beta titanium alloy Ti-4733 with different α phase morphologies was developed.
- The Ti-4733 alloy revealed more refined microstructures than the Ti-5553 resulting in enhanced tensile properties.
- The BASCA microstructures contain a combination of large lamellar α colonies, acicular α_s and discontinuous α_{GB} phases.
- The BASCA-processed Ti-4733 alloy exhibited a high elongation and relatively high strength.

GRAPHICAL ABSTRACT

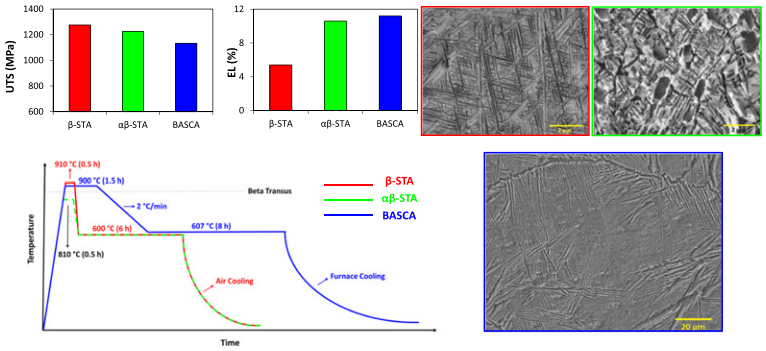

ARTICLE INFO

Article history:
Received 14 December 2016
Received in revised form 21 January 2017
Accepted 14 February 2017
Available online 16 February 2017

Keywords:
Beta titanium alloys
Alpha phase morphology
Tensile properties
Fracture

ABSTRACT

A novel beta titanium alloy Ti-4Al-7Mo-3Cr-3V (Ti-4733) was developed and the effect of its microstructure on the tensile properties was investigated and compared with the one of the commercial titanium alloy Ti-5553. Various alpha phase morphologies, namely globular, lamellar, acicular and a combination of them, were obtained as a result of the various heat treatments to which both the alloys were subjected. Although the alpha phase morphology for a given heat treatment was similar in both the alloys, the obtained microstructure was generally finer in the Ti-4733 alloy than in the Ti-5553 alloy, leading to enhanced tensile properties. The results showed that the microstructures with solely fine acicular alpha precipitates exhibited the highest tensile strength. While the highest reduction of area was derived in case of globular-acicular morphology, the maximum elongation was observed in microstructures containing lamellar-acicular alpha phase. Furthermore, for both the alloys the best balance between strength and ductility occurred in microstructures with a combination of globular and acicular alpha phase. The fractography analysis carried out on the tensile tested specimens showed a completely ductile fracture in case of globular-acicular morphology, ductile-transgranular brittle for lamellar-acicular morphology, and ductile-intergranular brittle for fully acicular α phase morphology.

1. Introduction

Near β and β titanium alloys have a great potential to be used in several fields, such as aerospace, biomedical and automotive industries as they offer high strength to weight ratios and very attractive combinations of strength, toughness and fatigue resistance [1,2]. The Ti-Al-Mo-

* Corresponding author at: Metallic Materials Research Center, Malek Ashtar University of Technology, Tehran, Iran.
E-mail address: sinsad64@yahoo.com (S. Sadeghpour).

http://dx.doi.org/10.1016/j.matdes.2017.02.043
0264-1275/

V-Cr composition is an important alloy system in which several β titanium alloys were introduced and used in commercial applications [3]. The most popular example is the Ti-5553 alloy that is a high strength β titanium alloy with chemical composition of Ti–5Al–5Mo–5V–3Cr (wt%). This alloy was primarily designed for high-strength forging applications as an improved version of the Russian alloy VT22 (Ti–5.7Al–5.1V–4.8Mo–1Cr–1Fe) on account of improved properties and deep hardenability over large thickness compared to the VT22. The Ti–5553 alloy proved also to be a better alternative than the Ti-10-2-3 alloy in some applications [3]. Beta titanium alloys are typically formed in the solution treated condition because they are ductile, with a low strength in the range 700–1000 MPa. They can subsequently be heat treated to gain very high strength levels up to 1200–1600 MPa. While the metastable β alloys generally display better cold workability when compared to α and α + β titanium alloys, unfortunately the cold workability of the most common high strength β titanium alloys, such as the Ti-5553, is not too high. This can be considered as a drawback for the Ti-5553 alloy restricting its application to bulk structures.

Recently, a new Ti-4Al-7Mo-3V-3Cr (Ti-4733) alloy, which contains almost the same primary alloying elements as the Ti-5553 alloy, was designed through the theoretical d-electron method with the aim of improving the alloy cold workability at room temperature [4]. This alloy was reported to exhibit high compressive strength (~1400 MPa) and excellent compressive deformability (~35%) in the solution treated condition. However, as a newly designed alloy, the effect of subsequent heat treatment on its microstructure and mechanical properties has not been studied yet as well as the correlation between the microstructure and the mechanical properties. In particular, it is worth to investigate if a higher level of strength can be achieved in this alloy, still preserving an acceptable ductility.

High levels of strength can be attained in the β titanium alloys through an aging heat treatment resulting in the precipitation of a fine secondary α phase [5]. Either the decrease in size or the increase in volume fraction of the secondary α phase improves the strength of the β titanium alloys [6]. However, in general, if the strength increases more than a certain level, the ductility may reduce. For example, the Ti-5553 alloy shows strengths up to 1517 MPa, but it is not used at this strength level due to its poor ductility [3]. On the other hand, the ductility is strongly dependent upon the prior β grain size, and reduces with increasing the solution temperature or the β grain size. In addition to the β grain size, the morphology of the primary α phase can affect the ductility of the β titanium alloys [7].

In addition to conventional solution treating and aging process, several heat treatment schedules have been designed in β titanium alloys to attain specific goals. For example, a particular processing method including Beta Annealing followed by Slow Cooling and Aging (BASCA) was developed to maximize the fracture toughness while maintaining a relatively high degree of strength in the conventional Ti-5553 alloy [8]. Although the microstructure and mechanical properties of the conventionally solution treated and aged Ti-5553 alloy have been vastly investigated over the past few years [3,9,10], the microstructural evolution during the BASCA process has not been studied systematically.

Table 1
Chemical composition of the investigated alloys (wt%).

Alloy	Al	Mo	V	Cr	Ti
Ti-4733	3.9	6.8	3.0	2.9	Balance
Ti-5553	5.2	4.8	4.7	2.9	Balance

The present work aims at studying the microstructural evolution of the Ti-4733 alloy as a result of different heat treatment cycles with an emphasis on the BASCA process and comparing them with the ones of the conventional Ti-5553 alloy. The effect of different microstructural morphologies on the mechanical properties of both the alloys is also critically discussed. This work provides an insight into the feasibility of attaining a good combination of strength and ductility in the Ti-4733 alloy and shows that this alloy can be a potential candidate to extend the engineering applications of the Ti-5553 alloy.

2. Experimental procedure

The new β titanium alloy Ti-4Al-7Mo-3V-3Cr (Ti-4733) was designed based on the commercial β titanium alloy known as Ti-5553 with the aim of controlling the cold deformation mechanisms. The details of alloy design strategy were presented elsewhere [4].

Ti-4733 and Ti-5553 ingots were melted twice by vacuum arc melting process to ensure chemical homogeneity. The ingots were prepared by melting pure elements. The ingots were then forged at 1100 °C and subsequently rolled to a 20-mm thick plate at 750 °C. The microstructure of the as-rolled alloys is shown in Fig. 1. The microstructures consist of both α and β phases in a deformed and elongated shape. The chemical composition of the alloys is given in Table 1. The β transition temperature (T_β) of the Ti-4733 and Ti-5553 alloys measured by metallographic method are 860 and 870 °C, respectively.

Samples were cut from both the alloys and five heat treatment cycles, namely β solution treatment (β-ST), α/β solution treatment (αβ-ST), β solution treatment and aging (β-STA), α/β solution treatment and aging (αβ-STA), and BASCA, were carried out on them. The schemes of these heat treatment cycles are shown in Fig. 2. All the heat treatment cycles were conducted in the electric resistance furnace in air. The solution treatments were performed at 810 °C (50 °C below the T_β) and

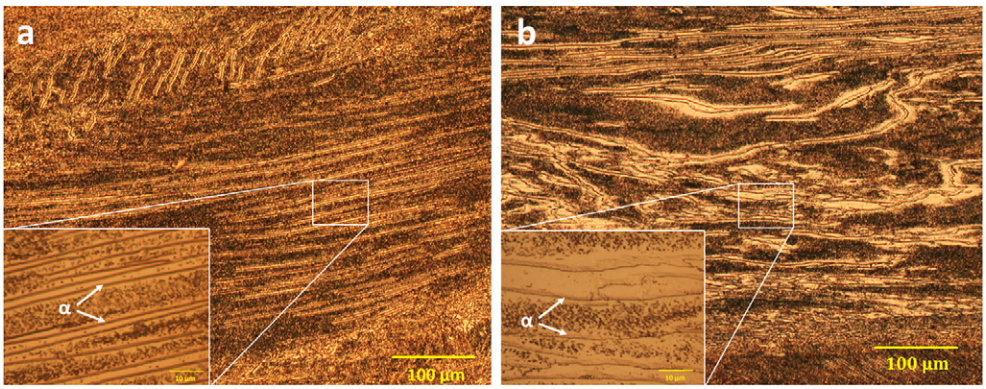

Fig. 1. Optical microstructure of the as-rolled specimens for the a) Ti-4733 and b) Ti-5553 alloys.

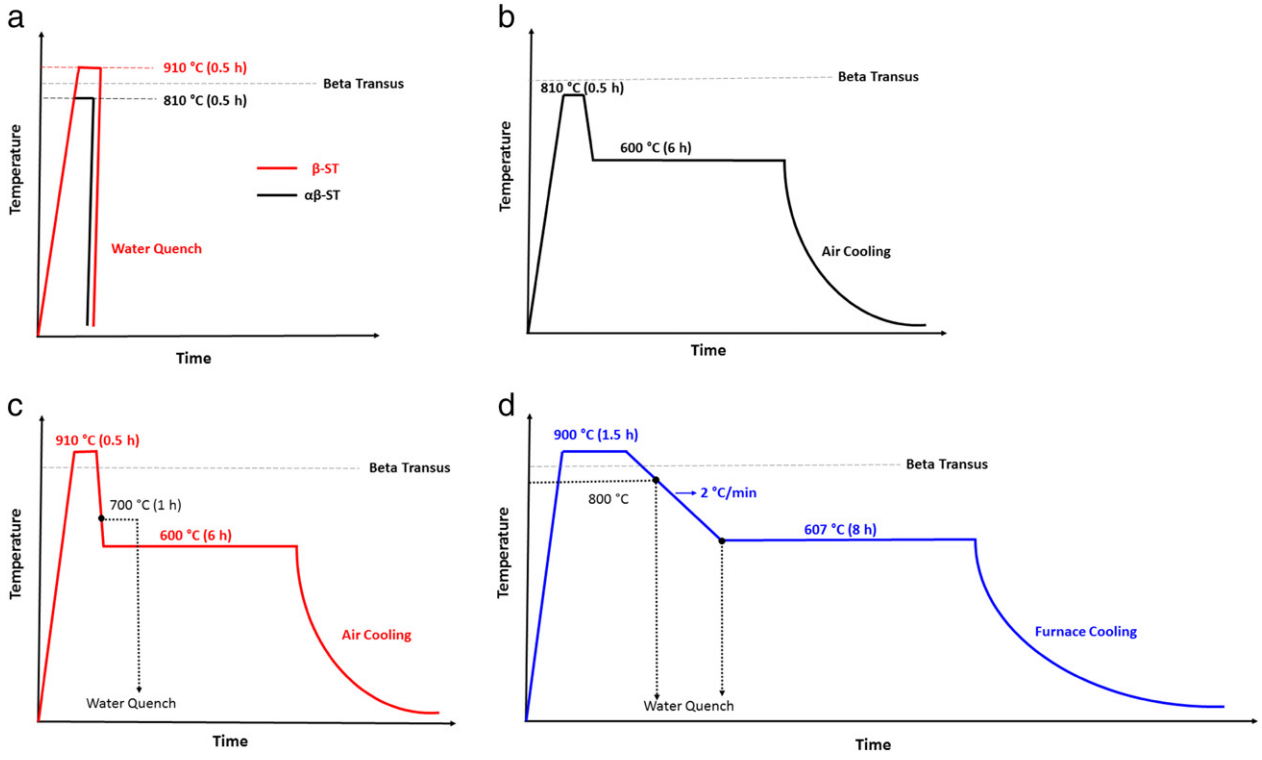

Fig. 2. Scheme of the heat treatment cycles applied in this study a) αβ-ST and β-ST b) αβ-STA c) β-STA and d) BASCA.

910 °C (50 °C above the T_β) for 30 min, followed by water quenching. For both the alloys the solution treatments were performed in a same condition. As shown in Fig.2(b and c), the STA process consisted of two stages of solution treatment at αβ or β phase regions followed by aging at 600 °C for 6 h. For this purpose, two furnaces were used, namely one for the solution treatment and another for the aging. This means that after the solution treatment in the first furnace, the samples were quickly placed (step cooled) in the second furnace set at the aging temperature. The average cooling rate from the solution temperature to the aging one was measured to be approximately 25 °C/s. To investigate the effect of the aging temperature on the morphology of the secondary α phase, one of the specimens was step cooled to 700 °C, and after holding at this temperature for 60 min water quenched (Fig. 2c).

The BASCA parameters were selected according to the original process introduced by Boeing for processing large components of airplanes aiming at improving the part fracture toughness [8]. As seen in the scheme of the BASCA heat treatment in Fig. 2(d), the samples were heated up to 900 °C and, after holding at this temperature for 1.5 h, slowly (2 °C/min) cooled down to 607 °C. After holding at 607 °C for 8 h, the samples were furnace cooled down to room temperature. To investigate the microstructure evolution during the BASCA process, two specimens were quenched in water after slow cooling down to 800 and 600 °C, respectively (Fig. 2d).

The specimens for microstructure observations were polished with 80–3000 grid SiC paper in water, followed by chemical polishing. A modified Kroll's reagent (6 ml HF + 18 ml HNO_3 + 76 ml H_2O) was employed to reveal the microstructures. The microstructural observations were carried out on an optical Olympus microscope and a TESCAN, MIRA3 Scanning Electron Microscope (SEM) in back scattered electron (BSE) and secondary electron (SE) imaging modes. The electron microscope was operated at 20 kV. The area fraction of the α phase was measured using the Clemex image analysis software. The calculation was performed based on several SEM micrographs from different positions of each sample.

The mechanical properties were evaluated by uniaxial tensile testing of ASTM-E8 standard specimens at room temperature. Flat tensile specimens with gage length 25 mm, width 6 mm and thickness 3 mm were machined along the rolling direction. Tensile tests were carried out on an Instron 8502 testing machine at a constant cross-head speed of 2 mm/min so that the initial strain rate was $1.3 \times 10^{-3}\ s^{-1}$.

3. Results and discussion

3.1. Solution treated microstructures

The optical microstructures of the alloys in β-ST and αβ-ST conditions are shown in Fig. 3. It can be seen that the microstructure is fully recrystallized after the solution treatment above the beta transus temperature of the alloys. According to Fig. 3(a and b) both the alloys in the β-ST condition show a single β phase microstructure with large equiaxed grains estimated to be 148 μm and 135 μm for the Ti-4733 and Ti-5553 alloys, respectively. According to Eq. (1) [11], the molybdenum equivalent (Mo_{eq}) and, consequently, the beta transus temperature of Ti-4733 is lower than that of the Ti-5553 alloy, which is in agreement with the metallographic observation of T_β. It was reported [12] that for β titanium alloys the recrystallization temperature is close to T_β and with a decrease in T_β the recrystallization temperature decreases. Therefore, we expect a lower recrystallization temperature for the Ti-4733 alloy due to its lower T_β. The recrystallization of the deformed β grains is fully completed in both alloys in the β-ST condition, leading to an immediate grain growth. This can explain the difference in the grain size of the two β-ST alloys.

$$Mo_{eq} = 1.00[Mo] + 0.28[Nb] + 0.22[Ta] + 0.67[V] + 1.60[Cr] + 2.90[Fe] - 1.00[Al] \quad (1)$$

As shown in Fig. 3(c and d), after an α/β solution treatment the microstructure of the two alloys consists of small β grains (0.9 μm for the

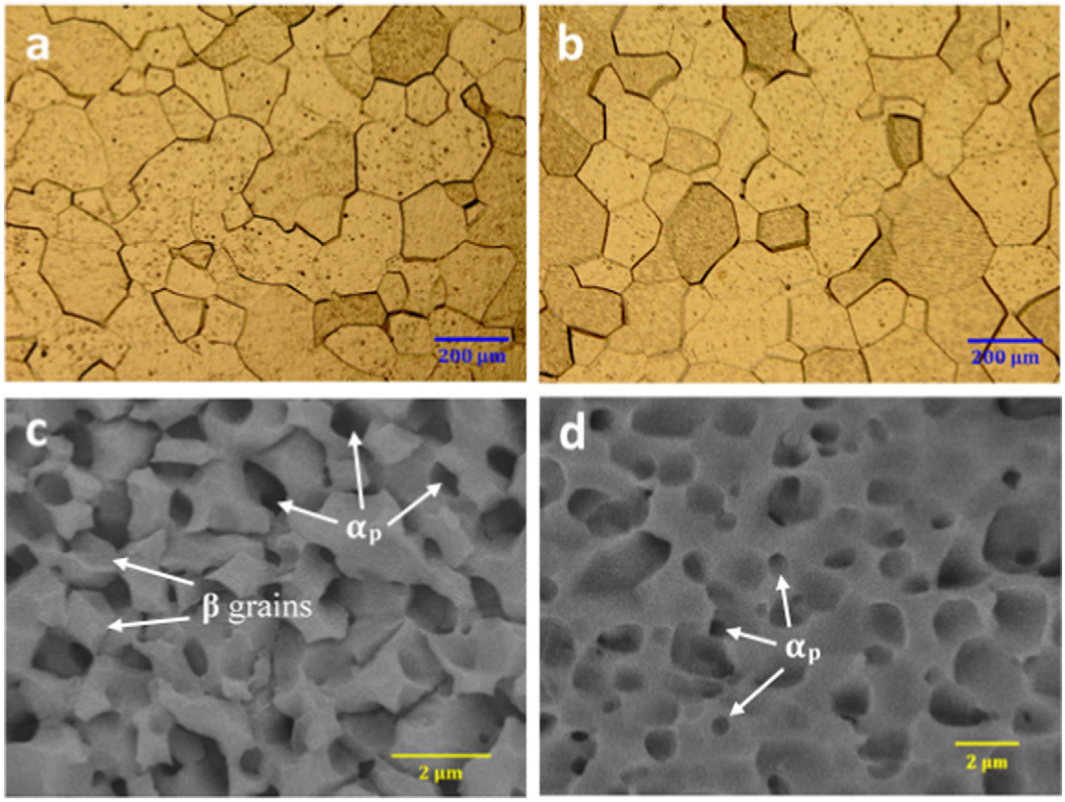

Fig. 3. Optical micrographs of the β-ST specimens for the a) Ti-4733 and b) Ti-5553 alloys and BSE SEM micrographs of the αβ-ST specimens for the c) Ti-4733 and d) Ti-5553 alloys.

Ti-4733 and 1.7 μm for the Ti-5553 alloy) and a significant amount of globular primary α (α_p) phases. The globular α_p phases have 0.5 μm and 1 μm average diameter in the Ti-4733 and Ti-5553 alloys, respectively. The volume fraction of the α_p phase after solution treatment at 810 °C for 30 min was found to be 32% for Ti-4733 and 26% for Ti-5553 (Table 2). In β titanium alloys, this type of microstructure can be obtained by processing them at T_β-50 °C to T_β-100 °C followed by α/β solution treatment [13]. Weiss and Ding et al. [14,15] showed that both the low and high angle sub-boundaries were formed across the α plates during hot working. Subsequent hot working provides a driving force that enables some β phase to penetrate into the α phase along the α/α sub-boundaries causing the separation into individual α grains [16]. The splitting of the sub-grains may be one of the fragmentation mechanisms for lamellar α leading to a globular morphology. The primary α phase located at the β grain boundaries (Fig. 3c) can limit the recrystallization and growth of the β phase due to its pinning effect. As mentioned before, the α_p particles in the Ti-4733 alloy have a smaller size and higher volume fraction than those in the Ti-5553 leading to more effective hindering of the grain growth and consequently smaller β grain size in the αβ-ST Ti-4733 alloy.

3.2. Solution treated and aged (STA) microstructures

The microstructures of the two alloys after the β-STA process are shown in Fig. 4. As it can be seen, the acicular α_s phases with a large aspect ratio formed during the aging. Since all the β grains are completely decorated with the α_s precipitates and there is no precipitation free zone through the microstructure of the β-STA specimens, it can be concluded that the precipitation process was completed. In the microstructures shown in Fig. 4, three variants of α precipitates arranged in form of triangles can be observed. This particular arrangement of α precipitates has often been associated with variant selection of the precipitates in order to accommodate the inherent as well as the transformational strains [17,18].

As seen in Fig. 4, the α_s precipitates in the Ti-5553 alloy (1–4 μm) are much longer compared to the Ti-4733 alloy (0.3–1 μm). According to Table 2, the average volume fraction of the α_s phase in the β-STA microstructure was found to be about 36% for Ti-4733 and 40% for Ti-5553. This may be attributed to the higher stability of the Ti-4733 alloy resulting in a reduced driving force for the nucleation and growth of the α_s phase during aging. The higher stability of the Ti-4733 alloy depends on its chemical composition, resulting in a lower transus temperature. According to Fig. 3(a and b), the β solution treatment results in coarse β grains without any primary α phase and, therefore, the least stable β matrix the greatest driving force will be available for its decomposition during the subsequent aging [19]. This leads to a faster secondary α (α_s) phase precipitation, meaning the α_s phases in β-STA samples would be coarser than those of the αβ-STA samples at similar aging conditions.

To investigate the effect of higher aging temperatures on the formation process of α phase, another type of heat treatment was applied, including solution treatment at β phase region and aging at 700 °C. In the Ti-4733 alloy sample step-cooled from 910 °C to 700 °C and aged only for 1 h at this temperature, considerable amounts of α precipitates with a totally different morphology can be observed (Fig. 5). According to Fig. 5, the α phase appears to form strings of aligned precipitates similar to the published results on the Ti-5553 alloy [20]. In this microstructure, prior β grain boundaries are decorated by serrated α precipitates (Fig. 5). Within the grains the mentioned strings are observed to have

Table 2
The volume fraction of the alpha phase in different microstructures.

Alloy	Volume fraction (%)	αβ-ST	β-STA	αβ-STA	BASCA
Ti-4733	Total α	31.6 ± 2	35.8 ± 1.5	49.2 ± 2.3	42.6 ± 1.7
	Secondary α	0	35.8 ± 1.5	17.5 ± 1.8	14.1 ± 1
Ti-5553	Total α	26.4 ± 1	40.4 ± 1.7	47.3 ± 2	51.9 ± 1.5
	Secondary α	0	40.4 ± 1.7	20.7 ± 1.5	14.4 ± 1.1

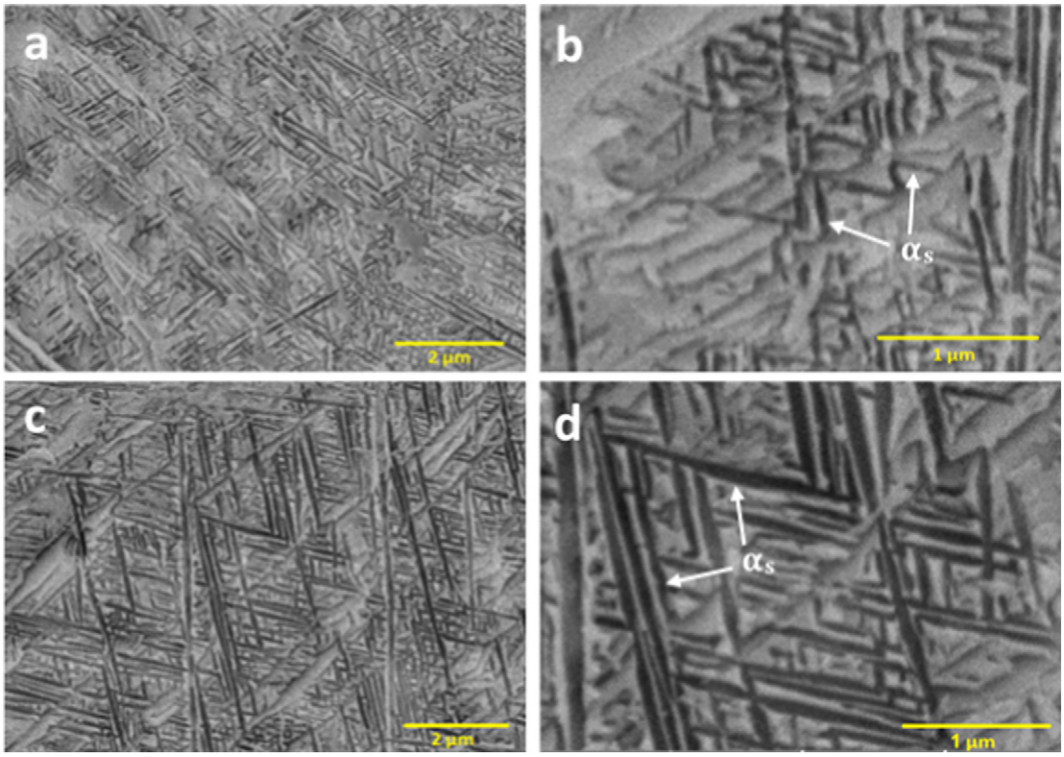

Fig. 4. BSE SEM micrographs of the β-STA specimens for the (a and b) Ti-4733 and (c and d) Ti-5553 alloys.

preferred morphological orientations. Three main string orientations with an angle of about 60° are visible in Fig. 5. As shown in Fig. 5 with arrow, the strings consist of individual α precipitates with a chevron like morphology. The two arms of the chevrons are approximately 1–3 μm in length.

In comparison to 700 °C, precipitates formed during aging at 600 °C are much finer (even after 6 h) and more densely distributed as well as have an absolutely different acicular morphology (Fig. 4). Even though more undercooling increases the driving force for nucleation of α phase and provides more nucleation sites, the observed change in the α phase morphology seems to be a result of other phenomena.

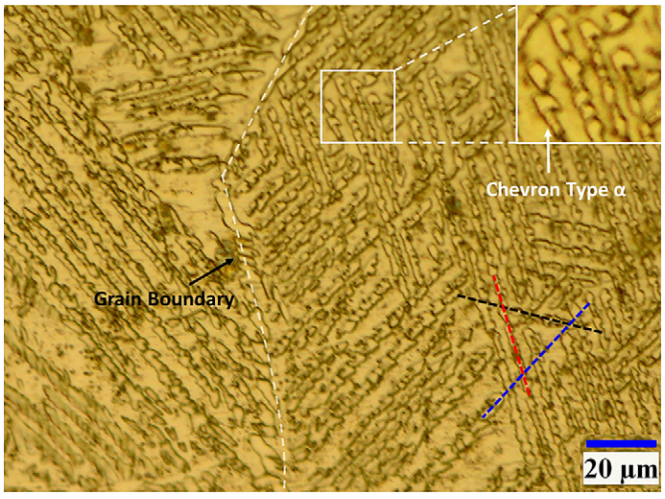

Fig. 5. Optical microstructure of the Ti-4733 alloy after step cooling from 910 °C to 700 °C, holding for 60 min and then water quenching.

Furthermore, in contrast to aging at 700 °C, there was no evidence of intergranular α_s growing in adjacent regions.

In previous literature [21,22] such an abrupt change in α phase morphology, volume fraction and growth kinetics was directly linked to the monotectoid reaction that occurs in some β titanium alloys. According to Nag [23], above and below the monotectoid isotherm, the α precipitates are in equilibrium with the solute lean and solute rich β phases, respectively. In order to maintain an overall mass balance, the volume fraction of α in equilibrium with the richer β phase has to be much more than that with the leaner β phase. Also, the fineness of the α precipitates below the monotectoid temperature suggests that the α nucleation could be assisted by the leaner phase. In β-STA conditions, the resulting microstructures indicate that a refinement took place during the aging below a certain temperature in the range of 600–700 °C. In fact, this temperature range seems to encompass a transition from larger string-like microstructure to a much more refined acicular α microstructure.

The microstructure of the two alloys after the αβ-STA condition are shown in Fig. 6. Similar to αβ-ST condition, in αβ-STA samples the primary α globules are present in the β matrix. Besides the globular α_p phases, the secondary α phases with acicular shape form during the aging. These α_s precipitates are usually of 0.2–0.5 μm in length, which are much finer than those of the β-STA specimens. The presence of α_p phase determines the stability of the remained β phase or the driving force for secondary α precipitation. The precipitation of primary α phase during the solution treatment below the T_β, results in a more stable remained β matrix. In fact, the effect of α_p precipitation is to enrich the β matrix by β stabilizer elements and to somehow deplete the α stabilizers. Therefore, the αβ solution treatment can lower the propensity of the remained β matrix to decompose and thus reduces the driving force for the α phase precipitation during the subsequent aging. Furthermore, the size of prior β grains (1.5 μm for Ti-4733 and 2.2 μm for Ti-5553 alloy) can also limit the maximum size of the α_s phases. Therefore, the small size of α_s precipitates in

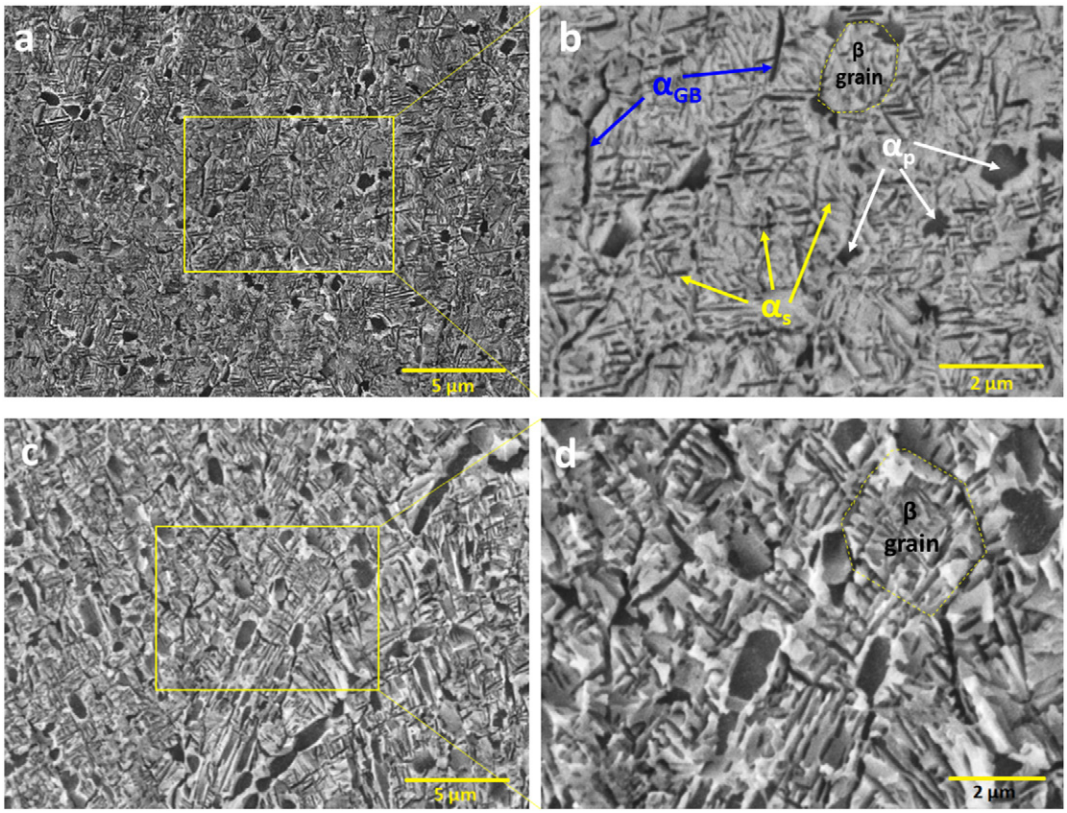

Fig. 6. SE SEM micrographs of the αβ-STA specimens for the (a and b) Ti-4733 and (c and d) Ti-5553 alloys.

αβ-STA specimens compared with β-STA specimens can be described based on the above scenario. It is also obvious from Fig. 6 and that the α_s precipitates in the Ti-4733 alloy are much finer than those in the Ti-5553 which similar to β-STA condition can be contributed to higher stability of the Ti-4733 alloy. Furthermore, the higher stability of the β phase after the αβ solution treatment of the Ti-4733 alloy leads a lower

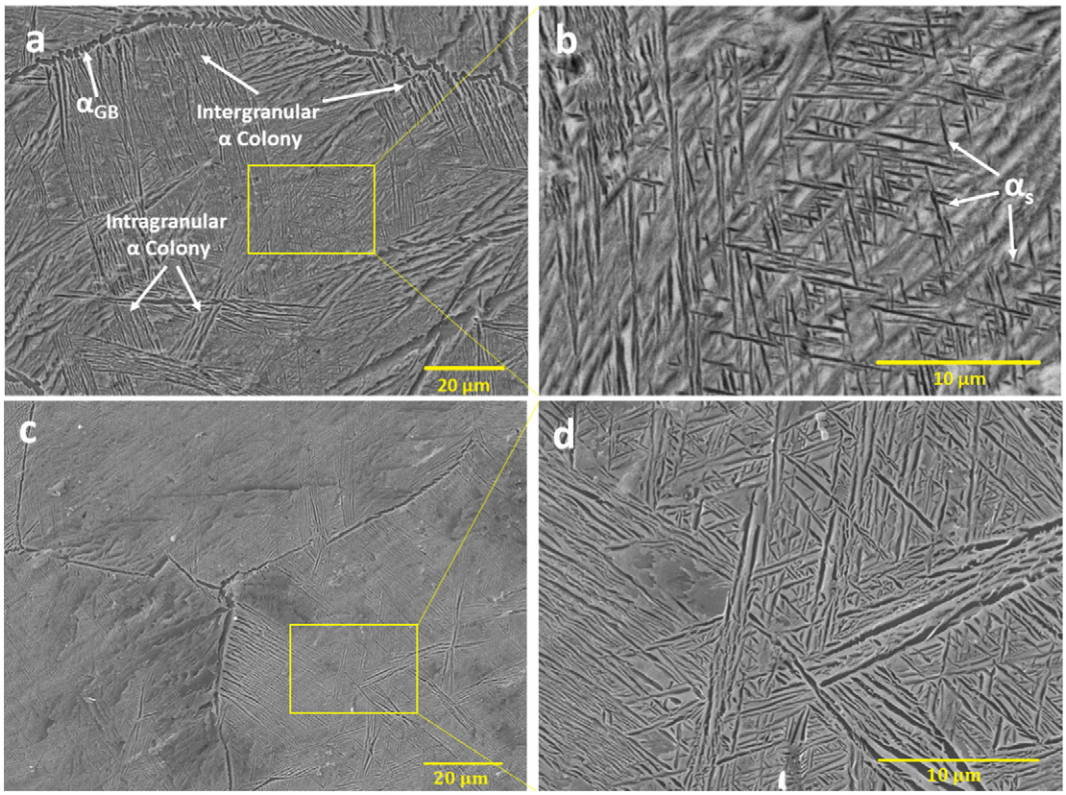

Fig. 7. SE SEM micrographs of the BASCA specimens for the (a and b) Ti-4733 and (c and d) Ti-5553 alloys.

volume fraction of the α_s phase to precipitate in the αβ-STA sample (Table 2).

3.3. Beta annealed, slow cooled and aged (BASCA) microstructures

The SEM micrographs of the two alloys after BASCA process are shown in Fig. 7. The lamellar inter and intra-granular α phases as colonies with different morphological orientations along with discontinuous grain boundary α (α_{GB}), are observed in the BASCA microstructures. Also, there are some fine α_s precipitates with acicular morphology between the primary α colonies.

By comparing the microstructures of the Ti-4733 and Ti-5553 alloys in Fig. 7, it is observed that the BASCA-treated Ti-4733 alloy tends to have more refined microstructure with a lower volume fraction of the α phase compared with Ti-5553 alloy (Table 2). This could be a result of the higher stability of the Ti-4733 alloy.

To investigate the microstructural evolutions during the BASCA heat treatment, samples from different stages of this process were analyzed. Slow cooling from solution temperature is a critical part of the BASCA process because can result in the formation of large α laths. To observe the effect of a slow cooling rate, specimens were cooled to 800 °C and 600 °C at a rate of 2 °C/min after annealing at 900 °C.

Fig. 8 shows the optical microstructure of the Ti-4733 alloy after slow cooling to 800 °C. It can be seen that the β grain boundaries are decorated by globular α precipitates acting as a precursor for nucleation and growth of intergranular α laths. These lamellar side plates form by branching out from α_{GB} globes as shown in Fig. 8b. No lamellar α plates nucleating directly on β/β grain boundaries were detected in the microstructure. In fact, the formation of lamellar α colonies is not possible without the presence of a parent α_{GB}. This observation is in accordance with a previous literature work [24]. These intergranular plates grow in a group resulting in the formation of a colony of parallel α plates. Higher magnification in Fig. 8(b) shows that α laths are not always present at both sides of the grain boundaries. Such orientation relationships between the α laths and β grains have already been observed in the Ti-5553 alloy [23] and in some α/β titanium alloys [25]. Some intragranular plates also nucleate in the interior of the β grains and grow as a group of parallel plates remaining stacked in a parallel mode within a given packet.

At lower cooling rates, laths that nucleate early at higher temperatures coarsen with the temperature reduction. Fig. 8c shows the optical microstructure of a sample that was slow cooled from the solutionizing temperature to 600 °C and then water quenched. Its microstructure presents grain boundary α (α_{GB}) and large volumes of intergranular and intragranular α laths. Intergranular α laths are formed in the form of many parallel plates growing towards the grain interior. They have short length and don't form the large colonies observed in common α/β titanium alloys. Intragranular α phases are also observed within the β matrix as plates growing in three preferred orientations. Furthermore, as seen in Fig. 8(c), there are some regions within the β grains where no α precipitates are detected, pointing out that the equilibrium volume fraction of α has not yet been achieved by cooling down to 600 °C. Therefore, further aging at this temperature (around 600 °C) can lead to the α precipitation over the entire β matrix. It is important to note that, because of the slow diffusion at low temperatures, the nucleation of secondary α precipitates can only occur with long aging treatments at low temperatures such as 600 °C.

Based on the observations, the sequence of microstructural evolution during the BASCA process can be summarized as follows:

1) The globular α_{GB} precipitates form at the grain boundaries with starting the slow cooling from the solution temperature.
2) The intergranular α colonies initially nucleate on the α_{GB} grow inside the grains with a lamellar morphology.
3) The intragranular α colonies nucleate and grow inside the grains with lamellar morphology.
4) At the end of the cooling stage, there would be some precipitate free zones inside the grains. With aging at 607 °C for a long time, the α_s precipitates with acicular morphology form in these zones.

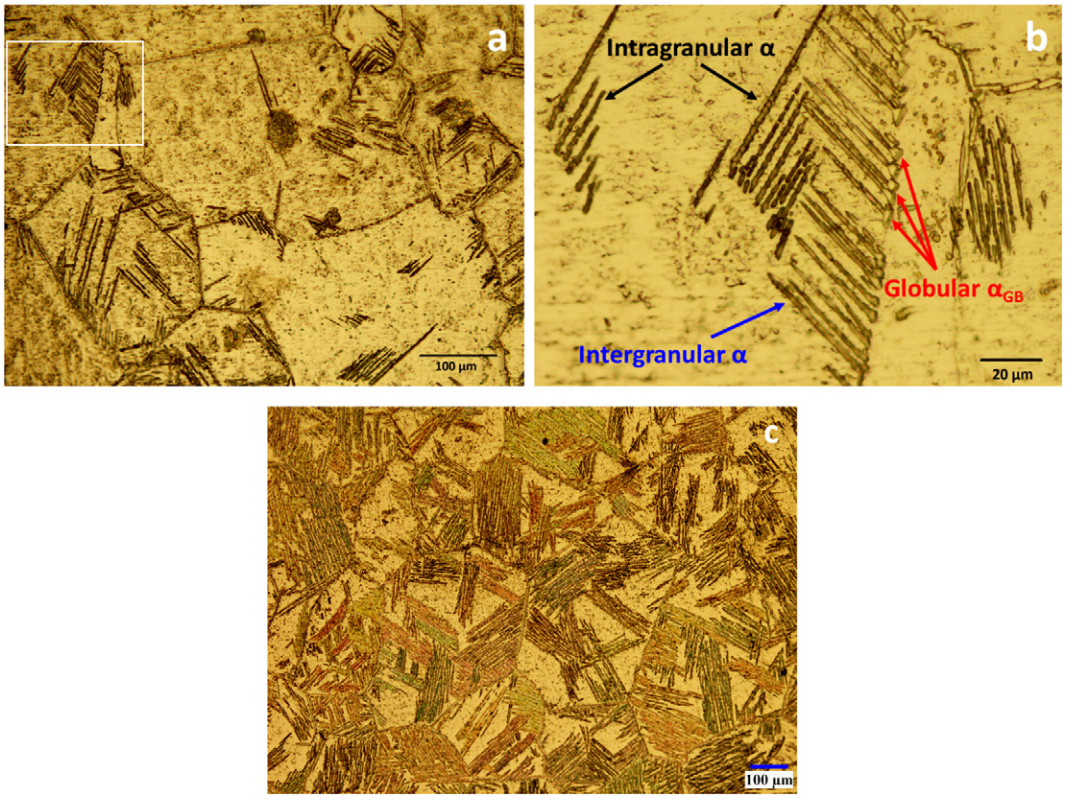

Fig. 8. Optical microstructure of the Ti-4733 alloy after slow cooling (2 °C/min) from 900 °C to (a and b) 800 °C, (c) 600 °C.

3.4. Mechanical properties

The tensile properties of the five different heat treatment conditions of the β-ST, αβ-ST, β-STA, αβ-STA and BASCA are shown in Fig. 9. As seen, both of the alloys exhibit a lower strength but higher ductility in the β-ST and αβ-ST conditions compared with the β-STA and αβ-STA conditions. Both of the alloys show higher strength and ductility in the αβ-ST condition than those in the β-ST samples. The higher strength of the αβ-ST samples is supposed to originate from the globular α_p phase which can lead to an increase in the strength. Furthermore, it has been reported [5] that the α_p phase has a direct influence on the ductility. In both solution treated conditions, the tensile properties of the Ti-4733 alloy are higher than those of the Ti-5553. Generally, the mechanical properties of a single β phase titanium alloy depend on the stability of the β phase determining its deformation mechanisms. It has been reported [26,27] that a combination of the slip and formation of the martensite improves the mechanical properties. The Ti-4733 alloy was developed in a way to exhibit the formation of deformation-induced martensite along with the dislocation slip as a combined deformation mechanism resulting in enhanced mechanical properties [4]. A detailed study on the design procedure and deformation mechanism of the Ti-4733 alloy in the single β phase condition can be found in Ref. [4]. However, due to the presence of the α phase in the αβ-ST condition, the stability of the β matrix is increased so that can lead to change in the deformation mechanism of β phase from the deformation-induced martensite to the slip. In fact, the tensile behavior of αβ-ST samples is mainly controlled by the α_p phase characteristics.

Generally, the deformation behavior of the α phase in a β titanium alloy and its effect on the mechanical properties is strongly dependent on its size and morphology. In β titanium alloys, the acicular α_s precipitates are much harder than the β phase because of their fine scale. These precipitates hardly deform and produce a high number of α/β interfaces act as dislocation barriers [28,29]. On the other hand, the lamellar α, α_p and α_{GB} phases are softer than the α_s and large enough to deform by slipping and shearing mechanisms so that the dislocations can be activated and accumulated within them [30]. It was recently demonstrated [30] that in large lamellar α phase, in addition to the slip of dislocations the twinning can be also activated during the deformation leading to an improved elongation of the lamellar microstructure during the tension. The highest yield strength of 1204 MPa and ultimate tensile strength of 1276 MPa are achieved in the Ti-4733 alloy and for the β-STA condition thanks to the developed fine acicular α_s phases. The fine α_s phase produced during the aging can act as a dislocation barrier leading to a significant increase in the alloy strength. As shown in Fig. 4, the width and length of the α_s precipitates in the Ti-4733 alloy are smaller than those in the Ti-5553 alloy. This difference in the α_s size arising from the higher stability of the Ti-4733 alloy, can explain why the Ti-4733 alloy shows a higher strength level in the β-STA condition. Meanwhile, the volume fraction of the α_s phase in the Ti-5553 alloy is higher than that of the Ti-4733 (Table 2). This indicates that the size of α_s precipitates, has a stronger effect on the strength than their volume fraction.

Although the β grain size in the β-STA specimens is quite larger than that of the αβ-STA specimens, the strength of the β-STA specimens is higher than that of the αβ-STA specimens. This can be attributed to the strong strengthening effect of the α_s precipitates in comparison with the β grain size effect. To this regard, some previous studies [32] showed that in the aged β titanium alloys the tensile strength can be considered independent from the β grain size. Furthermore, it is worth to mention that while the total volume fraction of the α phase in the αβ-STA microstructures is higher than that in the β-STA, the volume fraction of the α_s in the β-STA microstructures is higher (Table 2). This indicates that the α phase morphology has a more important role than its volume fraction in the strengthening of alloy.

As mentioned before, the solution treatment within the β phase region results in the least stable composition and the highest driving force for the precipitation of the α phase leading subsequently to large size of α_s. On the contrary, according to Fig. 6, for both the alloys the size of the α_s precipitates in the αβ-STA specimens (0.2–0.5 μm) is much finer than that of the β-STA specimens (1–4 μm). The solution treatment within the α/β phase region results in a more stable the β matrix and a reduced driving force for the nucleation and growth of the α phase during the subsequent aging.

It can be seen that for both the alloys the ductility of the αβ-STA specimens is higher than that of the β-STA specimens. The higher ductility of the αβ-STA specimens is attributed to the presence of the primary α phase. It was reported in [33] that the presence of α_p can improve the tensile ductility. In addition, the small sized prior the β grains give a contribution in improving the ductility of the αβ-STA specimens. The small β grain size can reduce the slip length and increase the

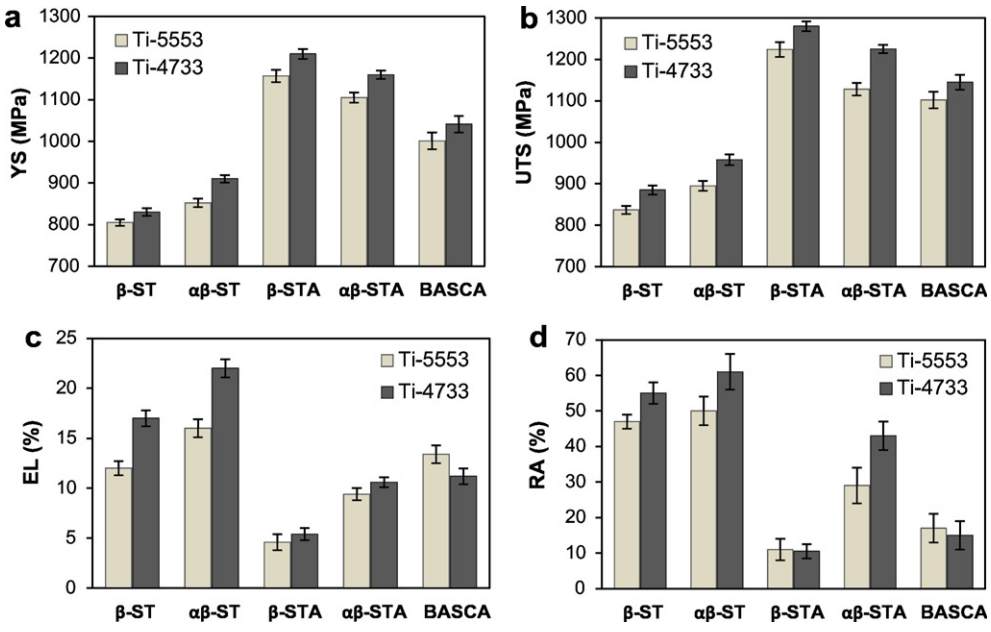

Fig. 9. Tensile properties of the Ti-4733 and Ti-5553 alloys including a) yield strength (YS), b) ultimate tensile strength (UTS), c) elongation to failure (EL) and d) reduction of area (RA) after the different heat treatment cycles.

crack nucleation resistance, thus improving the tensile ductility [34]. However, the strength level in the αβ-STA condition is relatively lower than that of the β-STA condition. This can be attributed to the reciprocal effect of the size and volume fraction of the secondary α phase in the αβ-STA and β-STA conditions. In the αβ-STA condition the microstructure contains both very fine acicular α_s precipitates, which have a significant effect on the strengthening, and large globular α_p phases with lower strengthening potential compared to the acicular α_s precipitates. In contrast, the β-STA microstructure contains only acicular α_s precipitates but with larger size than those of the αβ-STA. In fact, the size of the α_s precipitates and the volume fraction of the α_p phase, which are dependent on the solution treatment and aging conditions, determine the alloy final strength. In addition, the αβ-STA specimens tend to show an interesting tensile property balance (above 1200 MPa of ultimate strength with 10% of elongation).

According to Fig. 9c, in comparison to both the β-STA and αβ-STA conditions, the BASCA specimens exhibit higher elongation. This can be attributed to the coarse α-laths (Fig. 8c) resulting from the slow cooling employed in the BASCA process. According to Table 2 it can be seen that a considerable amount of the α phase in the BASCA samples is related to the lamellar α formed during the slow cooling. Although these coarse lamellar α phases can enhance the elongation of the BASCA specimens compared with the STA specimens, but they have a relatively poor hardening effect leading to lower strength levels. Despite the presence of coarse α-laths, the BASCA specimens show a tensile strength higher than 1100 MPa arising from the formation of secondary acicular α phases during the subsequent aging. In fact, the lamellar α phase determines the elongation of the BASCA specimens while the acicular α phase determines their strength. As shown in Fig. 9, the elongation of the Ti-5553 alloy in the BASCA condition is higher than that of the Ti-4733 that arises from its larger lamellar α phase and higher volume fraction of the lamellar α. However, with almost same volume fraction of the α_s precipitates, the strength of the Ti-5553 alloy is lower than that of the Ti-4733 because of its larger acicular α_s phase. However, it should be noted that these microstructural features are strongly dependent on the BASCA process parameters. In this study, we used the standard parameters of the Ti-5553 BASCA processing for both the alloys. Therefore, thanks to the optimization of the process parameters for the Ti-4733 alloy we may achieve even better mechanical properties.

It is worth to mention that despite the higher elongation of the BASCA specimens, these specimens show a lower reduction of area than that of the αβ-STA. The higher reduction of area in the αβ-STA condition may be attributed to the presence of globular α_p and small the β grain size providing more isotropic deformation behavior. In contrast, in the BASCA microstructure the lamellar α colonies form in a very large area (i.e. initial β grains) and are aligned in preferred orientations across all grains so that a high level of deformation heterogeneity can be occurred during the one-dimensional deformation. However, more detailed investigation should be done regarding the textural effect of the lamellar α on the mechanical anisotropy.

In addition, it can be concluded that in almost all heat treatment conditions, the Ti-4733 alloy exhibits higher mechanical properties compared with those of the Ti-5553. Meanwhile, the Ti-4733 alloy shows an enhanced cold deformability at room temperature in the single-phase solution treated condition [4]. This indicates that the Ti-4733 alloy can be used in applications including not only bulk structures but also plate or sheet products thanks to the achieved strength and ductility.

3.5. Fractography

To identify the effect of the α phase morphology on the fracture mechanisms, some solution treated and aged specimens were selected for the fractography analysis. Fig. 10 shows the fracture surface of the β-STA samples after the tensile test. As can be seen, both the alloys exhibit a mixed mode of intergranular brittle fracture with facet surfaces and intergranular cracks (as shown with arrows in Fig. 10a and c) besides minor ductile fracture with shallow dimples. Since the

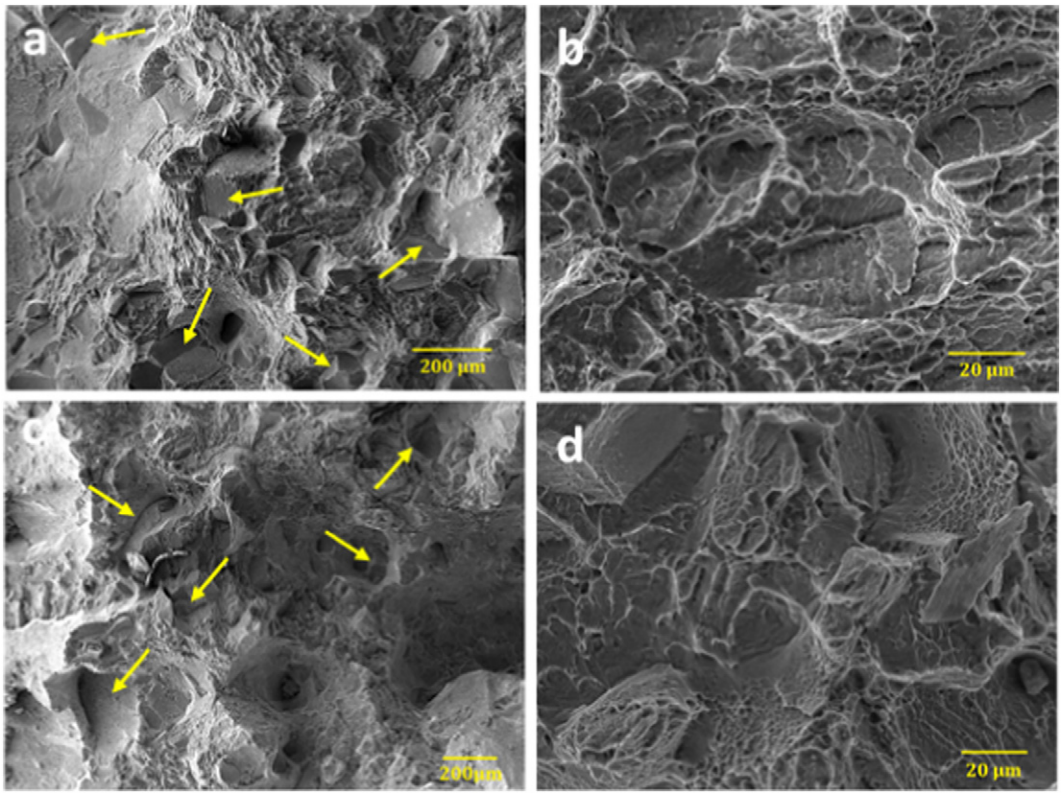

Fig. 10. Fracture surfaces of the (a and b) Ti-4733 and (c and d) Ti-5553 alloys in the β-STA condition.

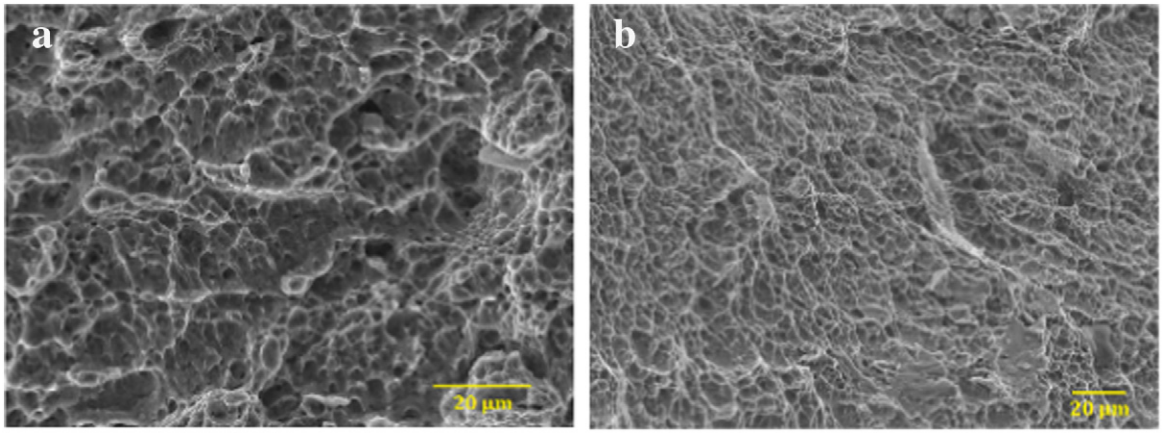

Fig. 11. Fracture surface of the (a) Ti-4733 and (b) Ti-5553 alloys in the αβ-STA condition.

strength of the α_s precipitates is higher than that of the β matrix, the strain in the β phase would be higher than in the α_s during deformation. This inhomogeneity in the strain can lead to the formation of micro-voids at the α/β interface. The micro-voids could coalescence and grow into the micro-cracks. This phenomenon was previously reported for the Ti-5553 alloy [31]. According to Fig. 10(b), the dimples are shallow and nonuniform in size. Since the α_s precipitates have different orientations relative to the loading axis during the tensile test, the voids associated with them can acquire very different sizes.

The lower ductility in the β-STA condition is due to the grain boundary α film and the large β grain size. The grain boundary α provides long soft zones that deform preferentially during deformation so that high stress concentrations and localized strains developed at triple junctions and resulted in separation of grains as shown in Fig. 10. Therefore, the intergranular brittle portion of the fracture surface is caused by the α_{GB} and large β grains while the ductile portion of the fracture surface results from the α_s precipitates.

Fractographs of the αβ-STA specimens in Fig. 11 show a completely ductile fracture mode. Fine and deep dimples associated with ductile fracture are visible in Fig. 11. It was showed that the dominant deformation mode for the αβ-STA condition is the strain localization in the matrix leading to voids at the interface between the aged matrix and the α_p phase. These voids could coalescence and grow up along the grain boundary of the α_p during the tensile test [7]. The cracks that initiate from the different α_p particles can meet each other by the shearing in the region between them. In fact, the α_p phase plays a key role in the fracture behavior of the αβ-STA microstructures. The reason is that the α_p phase can change the crack propagation direction.

It is worth to mention that although the α_{GB} is formed in the αβ-STA specimens (Fig. 6), the ductility is not reduced. The tensile ductility is

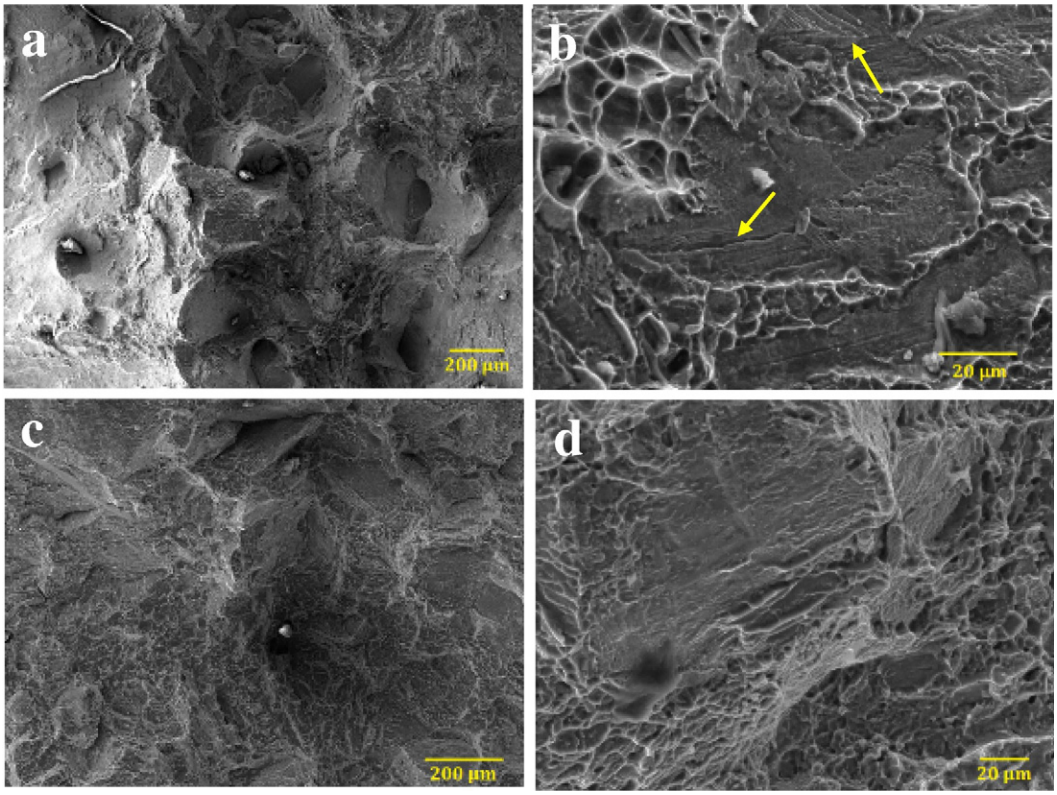

Fig. 12. Fracture surface of the (a and b) Ti-4733 and (c and d) Ti-5553 alloys in the BASCA condition.

mainly determined by the resistance to crack nucleation that is strongly dependent on the effective slip length parallel to the grain boundary α layers, and the small the β grain size of the αβ-STA microstructure can greatly reduce the slip length and therefore increase the crack nucleation resistance [35].

Fig. 12 shows the fracture surface of the BASCA samples after the tensile test. As can be seen, both the alloys exhibit a combination of ductile fracture with deep dimples and transgranular brittle fracture with some cracks (shown with arrows in Fig. 12b). It has been reported [38] that in the lamellar microstructures the cracks are much more liable to initiate at and propagate from the tips of thin microstructures that are the stress concentration regions. The high undulation depth on the fracture surface of the BASCA samples (Fig. 12), indicates the large deflection of crack path. In fact, the higher elongation of the BASCA samples compared with the STA samples arises from the presence of large lamellar α colonies. In general, the size of the lamellar α colonies, thickness of the α lamellae and size of the grain boundary α phase determine the alloy fracture behavior. In the Ti-5553 alloy, the lower stability of the β phase results in the growing of the α lamellar colonies, α lamellae and grain boundary α phase.

It is well known that the Ti-5553 alloy exhibits a higher fracture toughness when processed under BASCA conditions in compared to other processing routes, such as the conventional STA [8]. Although the fracture toughness of the samples was not measured in this study, some microstructural features can be useful to qualitatively describe the higher fracture toughness of the BASCA processed samples. It was showed that when the energy needed for the α lamellar fracture is higher than that needed for crossing colonies, the crack changes directions causing crack branching, zigzagging and secondary crack creation [36,37]. This process requires additional energy and can result in increased fracture toughness in the material [38].

The plastic zone of the crack tip is another factor in controlling the fracture behavior. The bigger the size of the plastic zone the higher the fracture toughness. According to Fan et al. [38] larger acicular α precipitates increase the plastic zone at the crack tip. They showed that the nucleation of dislocations from the crack tip across the smaller α phase leads to strain localization. Thus, it would significantly reduce the size of the plastic zone of the crack tip. The fact that the average size of the secondary α precipitates in the BASCA microstructure is much larger than that of the STA microstructures (Figs. 7, 6 and 4), can be another reason for the higher fracture toughness of the BASCA processed samples.

Generally, the α_{GB} has a critical importance due to its effect on the ductility [34,35,39]. Two aspects of α_{GB} can affect the fracture behavior of materials, namely its width and continuity [40]. As mentioned before (Fig. 7), there is a significant amount of α_{GB} phase in the microstructure of the BASCA samples. However, this α_{GB} phase exhibits a zigzag and discontinuous morphology as can be observed in Fig. 7. The discontinuity of the α_{GB} arises from the slow cooling during the BASCA process. In fact, during the slow cooling large and isolated globular α_{GB} particles form (Fig. 8b) and, subsequently, lead to a discontinuous grain boundary α phase. The propagation of crack will be more difficult through a discontinuous α layer compared to continuous α layer. Therefore, despite the presence of large amount of α_{GB}, it doesn't reduce the ductility significantly due to its discontinuous morphology. In addition, the three different and specific morphological aspects of large lamellar α colonies, larger acicular α_s precipitates and discontinuous α_{GB} are the main reasons of the higher fracture toughness in the BASCA microstructures.

4. Conclusions

In the present study, different morphologies of α phase were developed in a new beta titanium alloy, Ti-4733, through different heat treatments. Their microstructural evolution and effect on the tensile properties were investigated and compared with the ones of the commercial Ti-5553 alloy. The main results can be summarized as follows:

1) Although both the Ti-4733 and Ti-5553 alloys exhibit similar microstructures after a given heat treatment, in all the tested conditions the Ti-4733 alloy revealed more refined microstructures than the Ti-5553 resulting in enhanced tensile properties.
2) In the β-STA condition both the alloys exhibit a microstructure containing acicular α_s precipitates in the β matrix leading to high strength and low tensile ductility. The fractography of the β-STA specimens showed that the fracture mode was a combination of intergranular brittle and ductile fracture.
3) To achieve fine acicular α_s precipitates in the β-STA microstructures, the sample should be aged below the monotectoid temperature that is between 600 and 700 °C for the Ti-4733 alloy whereas aging above the monotectoid temperature results in a large chevron type α phase morphology.
4) In the αβ-STA condition both the alloys exhibit a bimodal microstructure with globular α_p and fine acicular α_s phases. The presence of these two morphologies results in good balance of strength and ductility. A completely dimpled ductile fracture was detected in the αβ-STA specimens.
5) The BASCA heat treatment results in a microstructure with combination of α_{GB} and lamellar α phase colonies formed during the slow cooling and fine acicular α_s precipitates formed during the subsequent aging. The BASCA-processed specimens exhibit a high elongation and relatively high strength. The fracture mode in BASCA specimens was found to be a combination of ductile and transgranular brittle fracture.

References

[1] O.M. Ivasishin, P.E. Markovsky, Y.V. Matviychuk, S.L. Semiatin, C.H. Ward, S. Fox, A comparative study of the mechanical properties of high-strength β-titanium alloys, J. Alloys Compd. 457 (1–2) (2008) 296–309.
[2] C. Leyens, M. Peters, Titanium and Titanium Alloys, Wiley-VCH, Cologne, 2003.
[3] S.L. Nyakana, J.C. Fanning, R.R. Boyer, Quick reference guide for β titanium alloys in the 00s, J. Mater. Eng. Perform. 14 (6) (2005) 799–811.
[4] S. Sadeghpour, S.M. Abbasi, M. Morakabati, Deformation-induced martensitic transformation in a new metastable β titanium alloy, J. Alloys Compd. 650 (2015) 22–29.
[5] C.-L. Li, X.-J. Mi, W.-J. Ye, S.-X. Hui, Y. Yu, W.-Q. Wang, Effect of solution temperature on microstructures and tensile properties of high strength Ti–6Cr–5Mo–5V–4Al alloy, Mater. Sci. Eng. A 578 (2013) 103–109.
[6] L. Mora, C. Quesne, R. Penelle, Relationships among thermomechanical treatments, microstructure, and tensile properties of a near beta-titanium alloy: β-CEZ: part II. Relationships between thermomechanical treatments and tensile properties, J. Mater. Res. 11 (01) (1996) 89–99.
[7] G.T. Terlinde, T.W. Duerig, J.C. Williams, Microstructure, tensile deformation and fracture in aged Ti-10V-2Fe-3Al, Metall. Trans. A. 14 (10) (1983) 2101–2115.
[8] R. Briggs, Tough, high-strength titanium alloys, Methods of Heat Treating Titanium Alloys, 2004 (inventor; Google Patents, assignee).
[9] S. Shekhar, R. Sarkar, S.K. Kar, A. Bhattacharjee, Effect of solution treatment and aging on microstructure and tensile properties of high strength β titanium alloy, Ti–5Al–5V–5Mo–3Cr, Mater. Des. 66 (Part B) (2015) 596–610.
[10] S.K. Kar, A. Ghosh, N. Fulzele, A. Bhattacharjee, Quantitative microstructural characterization of a near beta Ti alloy, Ti-5553 under different processing conditions, Mater. Charact. 81 (2013) 37–48.
[11] P. Bania, Beta titanium alloys and their role in the titanium industry, JOM 46 (7) (1994) 16–19.
[12] O.M. Ivasishin, P.E. Markovsky, Y.V. Matviychuk, S.L. Semiatin, Precipitation and recrystallization behavior of beta titanium alloys during continuous heat treatment, Metall. Mater. Trans. A 34 (2003) 147–158.
[13] Effect of thermomechanical processing on evolution of a phase morphology in b titanium alloys, in: A. Bhattacharjee, A. Joshi Vydehi, S.M. Hussain, A.K. Gogia (Eds.), Titanium 99: Science and Technology, CRISM, Prometey, Petersburg, 2000.
[14] R. Ding, Z.X. Guo, A. Wilson, Microstructural evolution of a Ti–6Al–4V alloy during thermomechanical processing, Mater. Sci. Eng. A 327 (2) (2002) 233–245.
[15] I. Weiss, F.H. Froes, D. Eylon, G.E. Welsch, Modification of alpha morphology in Ti-6Al-4V by thermomechanical processing, Metall. Trans. A. 17 (11) (1986) 1935–1947.
[16] Evolution of the equiaxed morphology of phases in Ti–6Al–4V, in: H. Margolin, P. Cohen (Eds.),Titanium 80: Science and Technology, 1980 (Japan, Kyoto).
[17] T. Furuhara, T. Maki, Variant selection in heterogeneous nucleation on defects in diffusional phase transformation and precipitation, Mater. Sci. Eng. A 312 (1–2) (2001) 145–154.
[18] S.C. Wang, M. Aindow, M.J. Starink, Effect of self-accommodation on α/α boundary populations in pure titanium, Acta Mater. 51 (9) (2003) 2485–2503.
[19] T.W. Duerig, J.C. Williams (Eds.), Beta Titanium Alloys in the 80's, The Minerals, Metals & Materials Society, Warrendale, PA, 1984.
[20] N.G. Jones, R.J. Dashwood, M. Jackson, D. Dye, Development of chevron-shaped α precipitates in Ti–5Al–5Mo–5V–3Cr, Scr. Mater. 60 (7) (2009) 571–573.

[21] T. Furuhara, T. Makino, Y. Idei, H. Ishigaki, A. Takada, T. Maki, Morphology and crystallography of α precipitates in β Ti-Mo binary alloys, Mater. Trans. JIM 39 (1) (1998) 31–39.
[22] E.S.K. Menon, H.I. Aaronson, Black plate formation in Ti-X alloys, Acta Metall. 34 (10) (1986) 1963–1973.
[23] S. Nag, Influence of beta instabilities on the early stages of nucleation and growth of alpha in beta titanium alloys (PhD thesis): The Ohio State University, 2008.
[24] M. Salib, J. Teixeira, L. Germain, E. Lamielle, N. Gey, E. Aeby-Gautier, Influence of transformation temperature on microtexture formation associated with α precipitation at β grain boundaries in a β metastable titanium alloy, Acta Mater. 61 (2013) 3758–3768.
[25] D. Bhattacharyya, G.B. Viswanathan, R. Denkenberger, D. Furrer, H.L. Fraser, The role of crystallographic and geometrical relationships between α and β phases in an α/β titanium alloy, Acta Mater. 51 (16) (2003) 4679–4691.
[26] T. Grosdidier, C. Roubaud, M.J. Philippe, Y. Combres, The deformation mechanisms in the β-metastable β-Cez titanium alloy, Scr. Mater. 36 (1997) 21–28.
[27] A. Bhattacharjee, V.K. Varma, S.V. Kamat, A.K. Gogia, S. Bhargava, Influence of β grain size on tensile behavior and ductile fracture toughness of titanium alloy Ti-10V-2Fe-3Al, Metall. Mater. Trans. A 37 (2006) 1423–1433.
[28] J. Huang, Z. Wang, K. Xue, Cyclic deformation response and micromechanisms of Ti alloy Ti–5Al–5V–5Mo–3Cr–0.5Fe, Mater. Sci. Eng. A 528 (2011) 8723–8732.
[29] D. Qin, Y. Lu, D. Guo, L. Zheng, Q. Liu, L. Zhou, Tensile deformation and fracture of Ti–5Al–5V–5Mo–3Cr–1.5Zr–0.5Fe alloy at room temperature, Mater. Sci. Eng. A 587 (2013) 100–109.
[30] C. Huang, Y. Zhao, S. Xin, W. Zhou, Q. Li, W. Zeng, Effect of microstructure on tensile properties of Ti–5Al–5Mo–5V–3Cr–1Zr alloy, J. Alloys Compd. 693 (2017) 582–591.
[31] D. Qin, Y. Lu, Q. Liu, L. Zheng, L. Zhou, Transgranular shearing introduced brittlement of Ti–5Al–5V–5Mo–3Cr alloy with full lamellar structure at room temperature, Mater. Sci. Eng. A 572 (2013) 19–24.
[32] Strengthening capability of beta titanium alloys, in: Y. Kawabe, S. Muneki (Eds.),Beta Titanium Alloys in the 1990's, 1993 (Warrendale, PA).
[33] T. Wang, H. Guo, Y. Wang, X. Peng, Y. Zhao, Z. Yao, The effect of microstructure on tensile properties, deformation mechanisms and fracture models of TG6 high temperature titanium alloy, Mater. Sci. Eng. A 528 (6) (2011) 2370–2379.
[34] G. Lütjering, J. Albrecht, C. Sauer, T. Krull, The influence of soft, precipitate-free zones at grain boundaries in Ti and Al alloys on their fatigue and fracture behavior, Mater. Sci. Eng. A 468–470 (2007) 201–209.
[35] C. Sauer, G. Lütjering, Influence of α layers at β grain boundaries on mechanical properties of Ti-alloys, Mater. Sci. Eng. A 319–321 (2001) 393–397.
[36] D.-G. Lee, S. Lee, Y. Lee, Effect of precipitates on damping capacity and mechanical properties of Ti–6Al–4V alloy, Mater. Sci. Eng. A 486 (1–2) (2008) 19–26.
[37] M. Niinomi, T. Kobayashi, Fracture characteristics analysis related to the microstructures in titanium alloys, Mater. Sci. Eng. A 213 (1–2) (1996) 16–24.
[38] J.K. Fan, J.S. Li, H.C. Kou, K. Hua, B. Tang, The interrelationship of fracture toughness and microstructure in a new near β titanium alloy Ti–7Mo–3Nb–3Cr–3Al, Mater. Charact. 96 (2014) 93–99.
[39] J.W. Foltz, B. Welk, P.C. Collins, H.L. Fraser, J.C. Williams, Formation of grain boundary α in β Ti alloys: its role in deformation and fracture behavior of these alloys, Metall. Mater. Trans. A 42 (3) (2011) 645–650.
[40] A. Ghosh, S. Sivaprasad, A. Bhattacharjee, S.K. Kar, Microstructure–fracture toughness correlation in an aircraft structural component alloy Ti–5Al–5V–5Mo–3Cr, Mater. Sci. Eng. A 568 (2013) 61–67.